Radboud Repository

Radboud University Nijmegen

PDF hosted at the Radboud Repository of the Radboud University Nijmegen

The version of the following full text has not yet been defined or was untraceable and may differ from the publisher's version.

For additional information about this publication click this link.
http://hdl.handle.net/2066/32360

Please be advised that this information was generated on 2017-12-05 and may be subject to change.

Continuous Time Quantum Monte Carlo method for fermions

A. N. Rubtsov,[1] V. V. Savkin,[2] and A. I. Lichtenstein[3, *]

[1]*Department of Physics, Moscow State University, 119992 Moscow, Russia*
[2]*Institute of Theoretical Physics, University of Nijmegen, 6525 ED Nijmegen, The Netherlands*
[3]*Institute of Theoretical Physics, University of Hamburg, 20355 Hamburg, Germany*

We present a numerically exact continuous-time Quantum Monte Carlo algorithm for fermions with a general interaction non-local in space-time. The new determinantal grand-canonical scheme is based on a stochastic series expansion for the partition function in the interaction representation. The method is particularly applicable for multi-band, time-dependent correlations since it does not invoke the Hubbard-Stratonovich transformation. The test calculations for exactly solvable models, as well results for the Green function and for the time-dependent susceptibility of the multi-band super-symmetric model with a spin-flip interaction are discussed.

arXiv:cond-mat/0411344v2 [cond-mat.str-el] 7 Mar 2005

I. INTRODUCTION

The variety of quantum Monte Carlo (QMC) methods is the most universal tool for the numerical study of quantum many-body systems with strong correlations. So-called determinental Quantum Monte Carlo (QMC) scheme for fermionic systems appeared more than 20 years ago[1,2,3,4]. This scheme has became standard for the numerical investigation of physical models with strong interactions, as well as for quantum chemistry and nano-electronics. Although the first numerical attempts were made for model Hamiltonians with local interaction, the real systems are described by the many-particle action of a general form. For example many non-local matrix elements of the Coulomb interaction do not vanish in the problems of quantum chemistry[5] and solid state physics[6]. For realistic description of Kondo impurities like a cobalt atom on a metallic surface it is of crucial importance to use the spin and orbital rotationally invariant Coulomb vertex in the non-perturbative investigation of electronic structure. The recently developed dynamical mean-field theory (DMFT)[7] for correlated materials introduces a non-trivial frequency-dependent bath Green function. The extension[8] of the theory deals with an interaction that is non-local in time. Moreover, the same frequency dependent single-electron Green-function and retarded electron-electron interaction naturally appear in any electronic subsystem where the rest of system is integrated out. An interesting non-local effect due to off-diagonal exchange interactions may be responsible for the correlated superconductivity in the doped fullerens[9]. It is worth noting that the exchange mechanism often has an indirect origin (like the super-exchange) and the exchange terms can therefore be retarded.

The determinantal grand-canonical auxiliary-field scheme[1,2,3,4] is extensively used for interacting fermions, since other known QMC schemes (like stochastic series expansion in powers of Hamiltonian[11] or worm algorithms[12]) suffer from an unacceptably bad sign problem for this case. The following two points are essential for the determinantal QMC approach: first, the imaginary time is artificially discretized, and the Hubbard-Stratonovich transformation[13] is performed to decouple the fermionic degrees of freedom. After the decoupling, fermions can be integrated out, and Monte Carlo sampling should be performed in the space of auxiliary Hubbard-Stratonovich fields. Hirsch and Fye[3] proposed a so-called discrete Hubbard-Stratonovich transformation to improve the efficiency of original scheme. It is worth noting that for a system of N atoms the number of auxiliary fields scales $\propto N$ for the local (short-range) interaction and as N^2 for the long-range one. This makes the calculation rather ineffective for the non-local case. In fact the scheme is developed for the local interaction only.

The problem of systematic error due to the time discretization was addressed in several works. For bosonic quantum systems, the continuous time loop algorithm[16], worm diagrammatic world line Monte Carlo scheme[12], and continuous time path-integral QMC[17] overcame this problem. Recently a continuous-time modification of the fermionic QMC algorithm was proposed[18]. It is based on a series expansion for the partition function in the powers of interaction. The scheme is free from time-discretization errors but the Hubbard-Stratonovich transformation is still invoked. Therefore the number of auxiliary fields scales similarly as the discrete scheme, so that the method remains local.

The most serious problem of the QMC simulation for large systems and small temperatures is the sign problem[14] resulting in the exponential growth of computational time. This is a principal drawback of the QMC scheme[14], but it is system dependent. For relatively small clusters, in particular for the local DMFT scheme, the sign problem is not crucial[7,15]. If we consider any subsystem obtained by integrating out the rest of the system, the Gaussian part as well as the interaction for the new effective action are non-local in space-time. Unfortunately, as we pointed out, the non-locality of the interaction hampers the calculation because it is hard to simulate systems with a large number of auxiliary spins. It is nearly impossible to simulate a system with interactions that are non-local also in time, when the number of

spins is proportional to $(\beta N/\delta\tau)^2$ (β is inverse temperature, and $\delta\tau$ is a time-slice).

Recent developments in the field of interacting fermion systems[10] clearly require the construction of a new type of QMC scheme suitable for non-local, time-dependent interactions. In this paper we present a continuous-time quantum Monte Carlo (CT-QMC) algorithm which does not introduce any auxiliary-field variables. The principal advantages of the present algorithm are related to the different scaling of the computational time for non-local interactions. The scheme is particularly suitable for general multi-orbital Coulomb interactions. The paper is aimed at a general description of the algorithm and the estimation of the computation complexity. We present the results for test systems to show an adequacy of the method. Moreover, an analysis of a non-trivial multi-band rotationally-invariant model with a time-dependent interaction is performed. This model demonstrates the

main advantages of the numerical scheme. The paper is organized as follows. In Section II we discuss a general formalism. Section III contains several applications of CT-QMC scheme for simple systems in comparison with the exact solutions and results of the super-symmetric multi-band impurity problem. The conclusions are given in the Section IV.

II. FORMALISM

A. General principles

One can consider the partition function for the system with a pair interaction in the most general case which has the following form:

$$Z = \mathrm{Tr}\,T e^{-S}, \tag{1}$$
$$S = \int\int t_r^{r'} c_{r'}^\dagger c^r \, dr\, dr' + \int\int\int\int w_{r_1 r_2}^{r_1' r_2'} c_{r_1'}^\dagger c^{r_1} c_{r_2'}^\dagger c^{r_2} dr_1 dr_1' dr_2 dr_2'.$$

Here T is a time-ordering operator, $r = \{\tau, s, i\}$ is a combination of the continuous imaginary-time variable τ, spin orientation s and the discrete index i numbering the single-particle states in a lattice. Integration over dr implies the integral over τ and the sum over all lattice states and spin projections: $\int dr \equiv \sum_i \sum_s \int_0^\beta d\tau$.

One can now split S into two parts: the unperturbed action S_0 in a Gaussian form and an interaction W. We

introduce as well an additional quantity $\alpha_{r'}^r$, which can be in principle a function of time, spin, and the number of lattice state. The functions $\alpha_{r'}^r$ will later help us to minimize the sign problem and to optimize the algorithm. Thus up to an additive constant we have:

$$S = S_0 + W, \tag{2}$$
$$S_0 = \int\int \left(t_r^{r'} + \int\int \alpha_{r_2}^{r_2} (w_{r r_2}^{r' r_2'} + w_{r_2 r}^{r_2' r'}) dr_2 dr_2' \right) c_{r'}^\dagger c^r \, dr\, dr',$$
$$W = \int\int\int\int w_{r_1 r_2}^{r_1' r_2'} (c_{r_1'}^\dagger c^{r_1} - \alpha_{r_1'}^{r_1})(c_{r_2'}^\dagger c^{r_2} - \alpha_{r_2'}^{r_2}) dr_1 dr_1' dr_2 dr_2'.$$

Now we switch to the interaction representation and make the perturbation series expansion for the partition function Z assuming S_0 as an unperturbed action:

$$Z = \sum_{k=0}^\infty Z_k = \sum_{k=0}^\infty \int dr_1 \int dr_1' ... \int dr_{2k} \int dr_{2k}' \Omega_k(r_1, r_1', ..., r_{2k}, r_{2k}'), \tag{3}$$
$$\Omega_k = Z_0 \frac{(-1)^k}{k!} w_{r_1 r_2}^{r_1' r_2'} \cdot ... \cdot w_{r_{2k-1} r_{2k}}^{r_{2k-1}' r_{2k}'} D_{r_1' r_2' ... r_{2k}'}^{r_1 r_2 ... r_{2k}}.$$

Here $Z_0 = \mathrm{Tr}\,T e^{-S_0}$ is a partition function for the unperturbed system and

$$D_{r_1' ... r_{2k}'}^{r_1 ... r_{2k}} = < T(c_{r_1'}^\dagger c^{r_1} - \alpha_{r_1'}^{r_1}) \cdot ... \cdot (c_{r_{2k}'}^\dagger c^{r_{2k}} - \alpha_{r_{2k}'}^{r_{2k}}) > . \tag{4}$$

Hereafter the triangle brackets denote the average over the unperturbed system (for arbitrary operator A: $<$

$A >= Z_0^{-1}\mathrm{Tr}TAe^{-S_0}$). Since S_0 is Gaussian, one can apply Wick's theorem to transform (4). Thus $D_{r_1'...r_{2k}'}^{r_1...r_{2k}}$ is a determinant of a $2k \times 2k$ matrix which consists of the two-point bare Green functions $g_{0r'}^r = < Tc_{r'}^\dagger c^r >$ at $\alpha_{r'}^r = 0$. Obviously, for non-zero $\alpha_{r'}^r$

$$D_{r_1' r_2' ... r_{2k}'}^{r_1 r_2 ... r_{2k}} = \det ||g_{0r_j'}^{r_i} - \alpha_{r_j'}^{r_i}\delta_{ij}||; i, j = 1, ..., 2k, \quad (5)$$

where δ_{ij} is a delta-symbol.

Now we can express the two-point Green function for the system (1) using the perturbation series expansion (3). It reads:

$$G_{r'}^r \equiv Z^{-1} < Tc_{r'}^\dagger c^r e^{-W} >= \sum_k \int dr_1 \int dr_1' ... \int dr_{2k} g_{r'}^r(r_1, r_1', ..., r_{2k}')\Omega_k(r_1, r_1', ..., r_{2k}'), \quad (6)$$

where $g_{r'}^r(r_1, r_1', ..., r_{2k}')$ denotes the Green function for a general term of the series

$$g_{r'}^r(r_1, r_1', ..., r_{2k}') = (D_{r_1'...r_{2k}'}^{r_1...r_{2k}})^{-1} \times \quad (7)$$
$$\times < Tc_{r'}^\dagger c^r (c_{r_1'}^\dagger c^{r_1} - \alpha_{r_1'}^{r_1}) \cdot ... \cdot (c_{r_{2k}'}^\dagger c^{r_{2k}} - \alpha_{r_{2k}'}^{r_{2k}}) > .$$

Similarly, one can write formulas for other averages, for example the two-particle Green function.

An important property of the above formulas is that the integrands stay unchanged under the permutations $r_i, r_{i'}, r_{i+1}, r_{i'+1} \leftrightarrow r_j, r_{j'}, r_{j+1}, r_{j'+1}$ with any i, j. Therefore it is possible to introduce a quantity K, which we call "state of the system" and is a combination of the perturbation order k and an *unnumbered set* of k tetrades of coordinates. Now, denote $\Omega_K = k!\Omega_k$, where the factor $k!$ reflects all possible permutations of the arguments. For the Green functions, $k!$ in the nominator and denominator cancel each other, so that $g_K = g_k$.

In this notation,

$$Z = \int \Omega_K D[K], \quad (8)$$
$$G_{r'}^r = Z^{-1} \int g_K \Omega_K D[K],$$

where $\int D[K]$ means the summation by k and integration over all possible realizations of the above-mentioned unnumbered set at each k. One can check that the factorial factors are indeed taken into account correctly with this definition.

B. Convergence of the perturbation series

It is important to notice that the series expansion for an exponent *always* converges for the finite fermionic systems. A mathematically rigorous proof can be constructed for Hamiltonian systems. Indeed, the many-body fermionic Hamiltonians H_0 and W have a finite number of eigenstates that is 2^N, where N is the total number of electronic spin-orbitals in the system. Now one can observe that $\Omega_k < const \cdot W_{max}^k$, where W_{max} is the eigenvalue of W with a maximal modulus. This proves convergence of (3), because the $k!$ in the denominator

grows faster than the numerator. In our calculations for the non-Hamiltonian systems we also did not observe any indications of the divergence.

The crucial point of the proof is the finiteness of the number of states in the system. This is a particular peculiarity of fermions. For bosons, on other hand, one deals with a Hilbert space of an infinite dimensionality. Therefore series like (3) are known to be divergent even for the simplest case of a single classical anharmonic oscillator[24]. It is important to keep this in mind for possible extensions of the algorithm to the electron-phonon system and to the field models, since these systems are characterized by an infinite-order phase space.

It is also important to note that this convergence is related to the choice of the type of series expansion. Indeed, the series (3) contains *all* diagrams, including disconnected. In the analytical diagram-series expansion disconnected diagrams drop out of the calculation and the convergence radius for diagram-series expansion differs from that of Eq.(3).

For the purpose of real calculation, it is desirable to estimate which values of k contribute the most to Z. It follows from the formula (3) that

$$< k >=< W > . \quad (9)$$

This formula gives also a simple practical recipe for how to calculate $< W >$. For example, in an important case of the on-site Coulomb interaction, it gives information about the local density-density correlator.

C. Random walk in K-space

Although formula (8) looks rather formal, it exactly corresponds to the idea of the proposed CT-QMC scheme. We simulate a Markov random walk in a space of all possible K with a probability density $P_K \propto |\Omega_K|$ to visit each state. If such a simulation is implemented, obviously

$$G_{r'}^r = \overline{sg_{r'}^r}/\overline{s} \quad (10)$$

The overline here denotes a Monte Carlo averaging over the random walk, and $\overline{s} = \Omega_K/|\Omega_K|$ is an average sign.

Two kinds of trial steps are necessary: one should try either to increase or to decrease k by 1, and, respectively, to add or to remove the corresponding tetrad of "coordinates".

Suppose that we perform incremental and decremental steps with an equal probability. Consider a detailed balance between the states K and K', where K' is obtained by an addition of certain tetrad $r_{2k+1}, r'_{2k+1}, r_{2k+2}, r'_{2k+2}$ to K. It should be noted that $P(K)$ and $P(K')$ appear under integrals of different dimensionality, respectively k and $k + 4$. Therefore it is more correct to discuss the detailed balance between the state K and all K' with $r_{2k+1}, r'_{2k+1}, r_{2k+2}, r'_{2k+2}$ corresponding to a certain domain d^4r. The detailed balance condition reads

$$\frac{P_{K \to K'}}{P_{K' \to K}} = \frac{P_{K'} \, d^4r}{P_K}, \qquad (11)$$

where $P_{K \to K'}$ is a probability to arrive in K' after a single MC step from K.

In the incremental steps the proposition for the four new points should be generated randomly. Denote the probability density in this generation $p(r_{2k+1}, r'_{2k+1}, r_{2k+2}, r'_{2k+2})$. If this step is accepted with a conditional probability $p_{K \to K'}$, then

$$P_{K \to K'} = p_{K \to K'} p(r_{2k+1}, r'_{2k+1}, r_{2k+2}, r'_{2k+2}) d^4r. \quad (12)$$

For the decremental steps, it is natural to pick randomly one of the existing tetrades and consider its removal. So,

$$P_{K' \to K} = p_{K' \to K}/(k + 1). \qquad (13)$$

Therefore, one obtains the condition for acceptance probabilities:

$$\frac{p_{K' \to K}}{p_{K \to K'}} = \left| \frac{\Omega_K}{\Omega_{K'}} \right| (k + 1) p(r_{2k+1}, r'_{2k+1}, r_{2k+2}, r'_{2k+2}). \qquad (14)$$

In principle, one can choose different $p(w_{r_{2k+1} r_{2k+2}}^{r'_{2k+1} r'_{2k+2}})$, it is important only to preserve (14). We propose to use

$$p = ||w||^{-1} |w_{r_{2k+1} r_{2k+2}}^{r'_{2k+1} r'_{2k+2}}| \qquad (15)$$
$$||w|| = \int \int \int \int |w_{rR}^{r'R'}| dr dR dr' dR'$$

to generate new points in the incremental steps. Then the standard Metropolis acceptance criterion can be constructed using the ratio

$$\frac{||w||}{k+1} \cdot \left| \frac{D_{r'_1 \dots r'_{2k+2}}^{r_1 \dots r_{2k+2}}}{D_{r'_1 \dots r'_{2k}}^{r_1 \dots r_{2k}}} \right|, \qquad (16)$$

for the incremental steps and its inverse for the decremental ones.

In general, one may want also to add-remove several tetrades simultaneously. A thus organized random walk is illustrated by Figure 1. The same Figure presents a typical distribution diagram for a perturbation order k in QMC calculation.
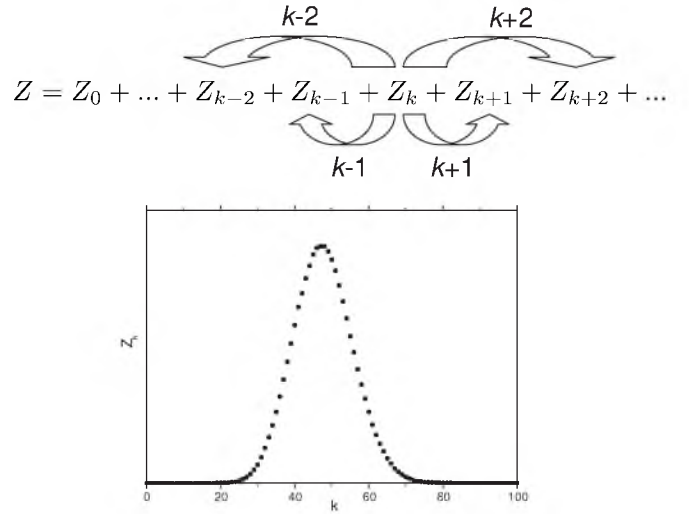
$$Z = Z_0 + \dots + Z_{k-2} + Z_{k-1} + Z_k + Z_{k+1} + Z_{k+2} + \dots$$

FIG. 1: Schematic picture of random walks in the space of $k; r_1, r'_1, \dots, r_{2k}, r'_{2k}$ according to perturbation series expansion (3) and an example of the histogram for the perturbation order k.

D. A fast-update of Green function matrix

The most time consuming operation of the algorithm is the calculation of the ratio of determinants and Green-function matrix. It's necessary for calculation of MC weights as well as for Green function.

There exist so called fast-update formulas for calculation of the ratio of determinants and Green-function matrix. Usual procedure takes N^3 operations, while the fast-update technique allows one to perform N^2 or less operations, where N is a matrix size.

Our derivation of the fast-update formulas is a generalization of the Shermann-Morrison scheme for the determinatal QMC. Usually, the two types of steps ($k \to k+1$ and $k \to k-1$) are sufficient. However, the steps $k \to k \pm 2$ can be also employed in certain cases (see later examples), so we present here also formulas for that case.

We use the following notation to derive the fast-update formulas:

$$R_{i,j} = G_{i,n} M_{n,j}, \qquad (17)$$
$$L_{i,j} = M_{i,n} G_{n,j},$$
$$M^{(k)} = D^{-1(k)},$$
$$\Delta = M^{-1(k+1)} - M^{-1(k)}.$$

Hereafter summation over repeated indices is implied and (k) denotes size of the matrix. In the last formulae matrix $M^{(k)}$ is extended to be a $(k + 1) \times (k + 1)$ matrix with $M_{k+1,k+1} = 1$ and $M_{k+1,i} = 0$, $M_{i,k+1} = 0$ (it does not change the ratio of determinants). Thus

$$M^{(k+1)} = M^{(k)}[1 + \Delta M^{(k)}]^{-1}, \qquad (18)$$
$$\frac{\det D^{(k+1)}}{\det D^{(k)}} = \frac{\det M^{(k)}}{\det M^{(k+1)}} = \det\left[1 + \Delta M^{(k)}\right] = \lambda.$$

Using the standard 2×2 super-matrix manipulations one

can obtain the following expression for $[1 + \Delta M^{(k)}]^{-1}$ matrix:

$$[1 + \Delta M^{(k)}]^{-1} = \begin{pmatrix} 1 + G_{1,k+1}\lambda^{-1}R_{k+1,1} & G_{1,k+1}\lambda^{-1}R_{k+1,2} & ... & G_{1,k+1}\lambda^{-1}R_{k+1,k} & -G_{1,k+1}\lambda^{-1} \\ G_{2,k+1}\lambda^{-1}R_{k+1,1} & 1 + G_{2,k+1}\lambda^{-1}R_{k+1,2} & ... & G_{2,k+1}\lambda^{-1}R_{k+1,k} & -G_{2,k+1}\lambda^{-1} \\ ... & ... & ... & ... & ... \\ G_{k,k+1}\lambda^{-1}R_{k+1,1} & G_{k,k+1}\lambda^{-1}R_{k+1,2} & ... & 1 + G_{k,k+1}\lambda^{-1}R_{k+1,k} & -G_{k,k+1}\lambda^{-1} \\ -\lambda^{-1}R_{k+1,1} & -\lambda^{-1}R_{k+1,2} & ... & -\lambda^{-1}R_{k+1,k} & \lambda^{-1} \end{pmatrix} \quad (19)$$

Then it's easy to the obtain fast-update formulas for the step $k+1$. Matrix $M^{(k+1)}$ can be obtained from $M^{(k)}$.

Finally the expressions for the matrix $M^{(k+1)}$ and for the ratio of determinants have the following form:

$$M^{(k+1)} = \begin{pmatrix} ... & ... & ... & -L_{1,k+1}\lambda^{-1} \\ ... & M'_{i,j} & ... & ... \\ ... & ... & ... & -L_{k,k+1}\lambda^{-1} \\ -\lambda^{-1}R_{k+1,1} & ... & -\lambda^{-1}R_{k+1,k} & \lambda^{-1} \end{pmatrix}, \quad (20)$$

$$M'_{i,j} = M^{(k)}_{i,j} + L_{i,k+1}\lambda^{-1}R_{k+1,j},$$

$$\frac{\det D^{(k+1)}}{\det D^{(k)}} = G_{k+1,k+1} - G_{k+1,i}M^{(k)}_{i,j}G_{j,k+1} = \lambda = \frac{1}{M^{(k+1)}_{k+1,k+1}},$$

where $i,j = 1,...,k$. For the step $k-1$ (removal of the column and row n) the fast update formulas for matrix $M^{(k-1)}$ and the ratio of determinants are as follows:

$$M^{(k-1)}_{i,j} = M^{(k)}_{i,j} - \frac{M^{(k)}_{i,n}M^{(k)}_{n,j}}{M^{(k)}_{n,n}}, \quad (21)$$

$$\frac{\det D^{(k-1)}}{\det D^{(k)}} = \frac{\det M^{(k)}}{\det M^{(k-1)}} = M^{(k)}_{n,n}.$$

One can also obtain fast-update formulas in the same

manner for steps $k \pm 2$. Let's introduce a 2×2 matrix λ:

$$\lambda_{q,q'} = G_{q,q'} - G_{q,i}M_{i,j}G_{j,q'}. \quad (22)$$

where $q,q' = k+1, k+2$. Then the fast-update formulas for a step $k+2$ look like

$$M^{(k+2)} = \begin{pmatrix} ... & ... & ... & -L_{1,q}\lambda^{-1}_{q,k+1} & -L_{1,q}\lambda^{-1}_{q,k+2} \\ ... & M'_{i,j} & ... & ... & ... \\ ... & ... & ... & -L_{k,q}\lambda^{-1}_{q,k+1} & -L_{k,q}\lambda^{-1}_{q,k+2} \\ -\lambda^{-1}_{k+1,q'}R_{q',1} & ... & -\lambda^{-1}_{k+1,q'}R_{q',k} & \lambda^{-1}_{k+1,k+1} & \lambda^{-1}_{k+1,k+2} \\ -\lambda^{-1}_{k+2,q'}R_{q',1} & ... & -\lambda^{-1}_{k+2,q'}R_{q',k} & \lambda^{-1}_{k+2,k+1} & \lambda^{-1}_{k+2,k+2} \end{pmatrix}, \quad (23)$$

$$M'_{i,j} = M^{(k)}_{i,j} + L_{i,q}\lambda^{-1}_{q,q'}R_{q',j},$$

$$\frac{\det D^{(k+2)}}{\det D^{(k)}} = \det \lambda,$$

where $i,j = 1,...,k$. For the step $k-2$ (removal of two columns and two rows $n+1, n+2$) matrix λ has the following form:

$$\lambda_{q,q'} = M_{q,q'}. \quad (24)$$

where $q,q' = n+1, n+2$. Then the fast update formulas for the matrix $M^{(k-2)}$ and the ratio of determinants are

as follows:

$$M_{i,j}^{(k-2)} = M_{i,j}^{(k)} - M_{i,q}^{(k)} \lambda_{q,q'}^{-1} M_{q',j}^{(k)}, \qquad (25)$$

$$\frac{\det D^{(k-2)}}{\det D^{(k)}} = \frac{\det M^{(k)}}{\det M^{(k-2)}} = \det[\lambda].$$

Using the fast update formula for ratio of determinants, the Green function can be obtained both in imaginary time and at Matsubara frequencies:

$$g_{\tau'}^{\tau} = g_{0\tau'}^{\tau} - \sum_{i,j} g_{0\tau_i}^{\tau} M_{i,j} g_{0\tau'}^{\tau_j}, \qquad (26)$$

$$g(i\omega) = g_0(i\omega) - g_0(i\omega)[\frac{1}{\beta} \sum_{i,j} M_{i,j} e^{i\omega(\tau_i - \tau_j)}] g_0(i\omega).$$

Here $g_0(i\omega)$ is a bare Green function.

Higher correlators can be obtained from Wick's theorem, just as in the auxiliary-field quantum Monte Carlo[3] scheme. Also note that it's convenient to keep in memory only the inverse matrices M instead of direct D in simulations.

E. The sign problem

A proper choice of α can completely suppress the sign problem in certain cases. To be concrete, let us consider a Hubbard model. In this model the interaction is local in time and space, and only electrons with opposite spins interact. Therefore it is reasonable to take $\alpha_{t'i'\uparrow}^{ti\uparrow} = \delta(\tau - \tau')\delta(i - i')\alpha_\uparrow$, similar for $\alpha_\downarrow$, and $\alpha_\uparrow^\downarrow = \alpha_\downarrow^\uparrow = 0$. The perturbation W becomes

$$W_{Hubbard} = U \int (n_\uparrow(\tau) - \alpha_\uparrow)(n_\downarrow(\tau) - \alpha_\downarrow)dt \qquad (27)$$

Here the Hubbard U and the occupation number operator $n = c^\dagger c$ are introduced. The Gaussian part of the Hubbard action is spin-independent and does not rotate spins. This means that only $g_\downarrow^\downarrow, g_\uparrow^\uparrow$ do not vanish, and the determinant in (5) is factorized

$$D_{r_1' r_2' \ldots r_{2k}'}^{r_1 r_2 \ldots r_{2k}} = D_{r_1' r_3' \ldots r_{2k-1}'}^{r_1 r_3 \ldots r_{2k-1}} D_{r_2' r_4' \ldots r_{2k}'}^{r_2 r_4 \ldots r_{2k}} \equiv D_\uparrow D_\downarrow \qquad (28)$$

For the case of attraction $U < 0$ one should choose

$$\alpha_\uparrow = \alpha_\downarrow = \alpha, \qquad (29)$$

where α is a real number. For this choice $g_\downarrow^\downarrow = g_\uparrow^\uparrow$, and therefore $D_\uparrow = D_\downarrow$. Ω is always positive in this case, as follows from formula (3).

This choice of α is useless for a system with repulsion, however. Compared to the case of attraction, another sign of w at $\alpha_\uparrow = \alpha_\downarrow$ results in alternating signs of Ω_k with odd and even k[20]. Another condition for α is required. The particle-hole symmetry can be exploited for the Hubbard model at half-filling. In this case, the transformation $c_\downarrow^\dagger \to \tilde{c}_\downarrow$ converts the Hamiltonian with repulsion to the same but with attraction. Therefore the series (3) in powers of $W = U \int (n_\uparrow(\tau) - \alpha)(\tilde{n}_\downarrow(\tau) - \alpha)dt$

does not contain negative numbers, in accordance to the previous paragraph. The value of the trace in (3) is independent of a particular representation. In the original (untransformed) basis the above W reads as $U \int (n_\uparrow(\tau) - \alpha)(n_\uparrow(\tau) - 1 + \alpha)dt$. We conclude that

$$\alpha_\uparrow = 1 - \alpha_\downarrow = \alpha \qquad (30)$$

eliminates the sign problem for repulsive systems with a particle-hole symmetry. Of course, the average sign for a system with repulsion is not equal to unity in a general case.

It is useful to analyze a toy single-atom Hubbard model to get a feeling for the behavior of the series (3). The two parts of the action are

$$S_0 = \int (-\mu + U\alpha_\downarrow)n_\uparrow(\tau) + (-\mu + U\alpha_\uparrow)n_\downarrow(\tau))d\tau; (31)$$
$$W = U \int (n_\downarrow(\tau) - \alpha_\downarrow)(n_\uparrow(\tau) - \alpha_\uparrow)d\tau.$$

Here μ is a chemical potential. For a half-filled system $\mu = U/2$. For this model, it is easy to calculate terms of the series for Z explicitly. We obtain

$$\Omega_k = \frac{(-U\alpha_\uparrow\alpha_\downarrow)^k}{k!} \left(1 + e^{\beta(\mu - U\alpha_\downarrow)}(1 - \alpha_\uparrow^{-1})^k\right) \times$$
$$\times \left(1 + e^{\beta(\mu - U\alpha_\uparrow)}(1 - \alpha_\downarrow^{-1})^k\right). \qquad (32)$$

Consider the case of repulsion ($U > 0$). Let us use the condition (30) for an arbitrary filling factor. The later expression can be presented in the form

$$\Omega_k = e^{\beta(\mu - U\alpha)} \frac{(U\alpha^2)^k}{k!} \left(1 + e^{\beta(\mu - U + U\alpha)}(1 - \alpha^{-1})^k\right) \times$$
$$\times \left(1 + e^{\beta(-\mu + U\alpha)}(1 - \alpha^{-1})^k\right). \qquad (33)$$

For $\mu = U/2$ the value of Ω_k is positive for any α. For a general filling factor, the situation depends on the value of α. For $0 < \alpha < 1$ negative numbers can occur at certain k. Outside this interval all terms are positive, and there is no sign problem for the single-atom system under consideration.

Since the sign problem exists already for the impurity problem for $0 < \alpha < 1$, such a choice is also not suitable for the N-atom repulsive Hubbard system. On the other hand, minimization of $\bar{W}$ requires α to be as close to this interval as possible. Therefore it is reasonable to take $\alpha = 1$ or slightly above. This is the same as zero or a small negative value, since $\alpha_\uparrow = 1 - \alpha_\downarrow$. We use the similar choice of α's for more complicated multi-orbital models and always obtain a reasonable average sign.

Finally, one may prefer to have a perturbation that is symmetrical in spin projections. Formula (29) for the attractive interaction is already symmetrical. For the case of repulsion we propose to use a symmetrized form

$$\frac{U}{2}(n_\uparrow + \alpha)(n_\downarrow - 1 - \alpha) + \frac{U}{2}(n_\uparrow - 1 - \alpha)(n_\downarrow + \alpha) \qquad (34)$$

with some small positive α.

There is another argumentation why the presence of α's in Eq. (34) is very important. Indeed, proper choice

of α make the average of Eq. (34) negative. We can call such an interaction "virtually attractive in average". It makes possible to obtain the k-series with the all-positive integrals in the expansion, whereas the same series without α's is useless due to the alternative signs of integrals. We believe that the similar reasoning is valid for the non-local interaction. Note however that the proper choice of the α's depends on the particular system under calculation. For now, we cannot offer a general recipe. In a certain situation, the expressions under the integrals are not always positive, and the exponential falloff occurs for the large systems or small temperature. The practical calculations of the average sign and comparison with the discrete-time QMC scheme are presented in the next Section.

III. APPLICATIONS OF CT-QMC METHOD

We test present algorithm for several well known models in this Section. These examples show some of the advantages of the CT-QMC method.

In all examples presented below we calculate a Green function at Matsubara frequencies $G(i\omega_n)$. Total number of Matsubara frequencies is varied from 10 to 20. The typical number of QMC trials is $10^6 \div 10^7$. Normally, the error bar of the CT-QMC data for $G(i\omega_n)$ is less than $3 \cdot 10^{-3}$ for the lowest Matsubara frequency and becomes smaller as frequency increases. Obviously, values of these typical parameters depend on concrete system.

A. Hubbard clusters

To test the scheme, we start from a single isolated Hubbard atom and a 2×2 Hubbard cluster. Results are compared with the known exact solution (see e.g. Ref. 7).

The solution for the atomic limit reads as follows:

$$G(i\omega) = \frac{1-n}{i\omega+\mu} + \frac{n}{i\omega+\mu-U},$$ (35)
$$n = (e^{\beta\mu} + e^{\beta(2\mu-U)})/(1 + 2e^{\beta\mu} + e^{\beta(2\mu-U)}).$$

Results for $U = 2, \beta = 16, \mu = U/2$ are presented in Figure 2. Thus CT-QMC data are in an excellent agreement with the analytical solution.

Further we apply CT-QMC algorithm to the 2×2 Hubbard lattice to compare with the auxiliary-field quantum Monte Carlo scheme[3]. We start with the half-filled case ($\mu = U/2$, four electrons in the system). It can be shown that for the particular case of half-filling one can choose $\alpha_\uparrow = \alpha_\downarrow = 0.5$ due to the particle-hole symmetry. Expression (9) for this case becomes $< k > = \beta N(0.5- < n_\uparrow n_\downarrow >)$ with $N = 4$. It can be verified that this choice delivers the minimal possible $< k >$. Series (3) contains only the terms with an even k in this case, so it's appropriate to use steps ± 2.
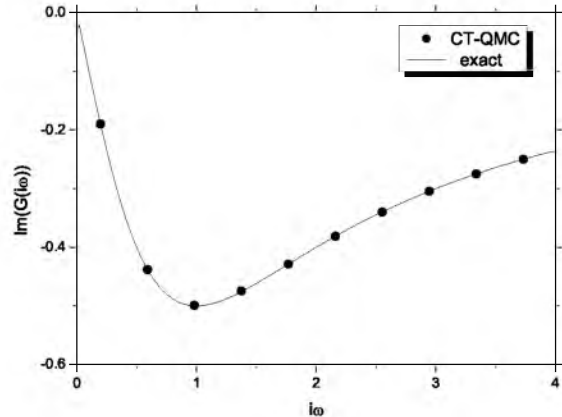

FIG. 2: Imaginary part of the Green function at Matsubara frequencies for a single atom with Hubbard repulsion U. Symbols are CT-QMC data, line is an exact solution[7]. Parameters: $U = 2, \beta = 16, \mu = U/2$. Error bar is less than symbol size.
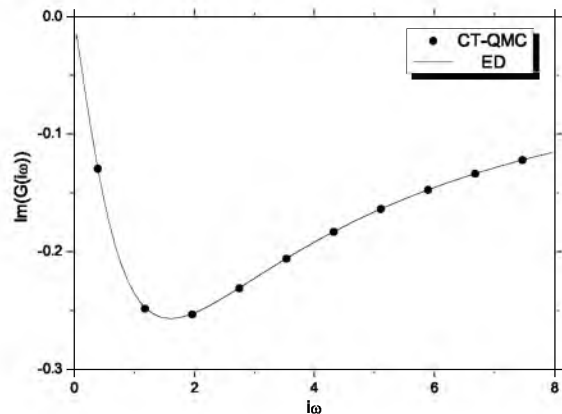

FIG. 3: 2×2 Hubbard lattice at half-filling. Imaginary part of the Green function at Matsubara frequencies: symbols are CT-QMC data, line is exact-diagonalization data. Parameters: $U = 4, t = 1, \beta = 8, \mu = U/2$. Error bar is less than symbol size.

Results for $U = 4, t = 1, \beta = 8$ in comparison with the exact-diagonalization data are shown in Figure 3.

Cases of a single atom and a half-filled cluster do not suffer a sign problem. One can discuss a sign problem considering 2×2 Hubbard lattice away from half-filling. For this case a choice (34) for α's was used. We concentrate on the worst sign-problem case when there are three electrons in the system[21]. The average sign is presented in Figure 4 as a function of inverse temperature β. We would like to stress that the CT-QMC algorithm agrees
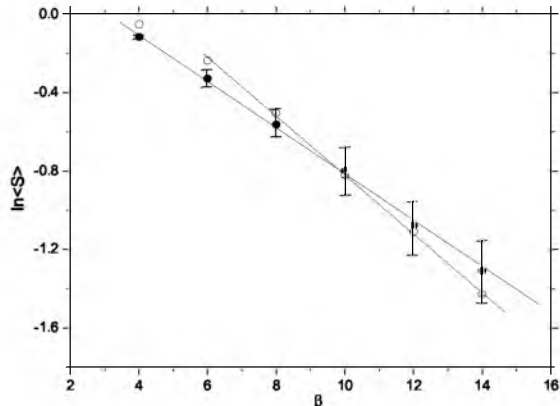
FIG. 4: 2×2 Hubbard lattice away from half-filling: three electrons in the system. Average sign as a function of β: CT-QMC (filled symbols) and auxiliary-field quantum Monte Carlo[3] (opened symbols) algorithms results. Lines are guides to the eye. Parameters: $U = 4, t = 1$.
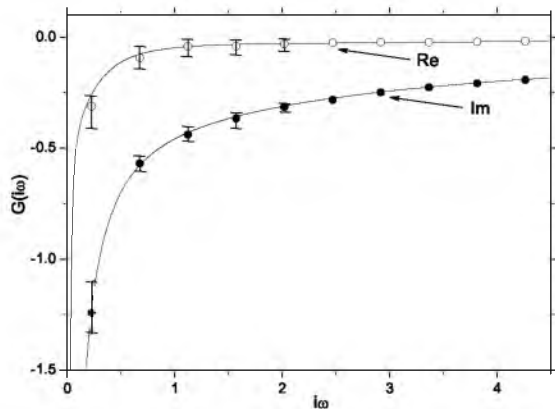

FIG. 5: Real and imaginary parts of the Green function for 2×2 Hubbard lattice away from half-filling: three electrons in the system. Parameters: $U = 4, t = 1, \beta = 14$. Symbols are CT-QMC data, lines are exact-diagonalization results. Error bar for $i\omega > 2$ is less than symbol size.

with the auxiliary-field quantum Monte Carlo[3] scheme (Figure 4). Even for a relatively small average sign, numerical data remain to be in a good agreement with the exact-diagonalization, as Figure 5 shows.

B. Metal-insulator transition on the Bethe lattice

One of the advantages of the CT-QMC algorithm is a possibility to perform simulations at lower temperatures

with higher accuracy than the auxiliary-field quantum Monte Carlo[3] method. Here we present results for the metal-insulator phase transition in Hubbard model on Bethe lattice[7]. The effective one-site problem based on the dynamical mean-field theory[7] is solved by CT-QMC method.

The standard self-consistent loop of DMFT equations is as follows[7]. One starts with some initial guess for the Green function $\mathcal{G}_0$ which is used to obtain the local Green function $\mathcal{G}$ from the effective action as[7]

$$\mathcal{G}(\tau, \tau') = < T c^\dagger_{\tau'} c^\tau >_{S_{eff}(\mathcal{G}_0)} . \tag{36}$$

A new guess for the Green function $\mathcal{G}_0$ is obtained from the equation for Bethe lattice $(t = 1/2)$[7]:

$$\mathcal{G}_0^{-1}(i\omega) = i\omega + \mu - t^2 \mathcal{G}(i\omega). \tag{37}$$

Formulas (36,37) form a self-consistent loop of DMFT equations. The Green function which corresponds to the semi-circular density of states with band-width 2 is usually used for the Bethe lattice:

$$\mathcal{G}_0(i\omega) = \frac{2}{i(\omega + \sqrt{\omega^2 + 1}) + 2\mu}. \tag{38}$$

The self-energy $\Sigma(i\omega)$ can be obtained from the following formula after the iteration procedure for the DMFT equations (36,37) has converged:

$$\Sigma(i\omega) = \mathcal{G}_0^{-1}(i\omega) - \mathcal{G}^{-1}(i\omega). \tag{39}$$

Results for the metal-insulator phase transition in Hubbard model on Bethe lattice at half-filling for $\beta = 64$ are presented in Figure 6. Local Green functions and corresponding self-energies are shown for values of Coulomb interaction U from the value $U = 2$ to the value $U = 3$ with the step $\Delta U = 0.2$. The results show a phase transition from the metallic state (smaller values of U) to the insulating state (larger values of U) with a coexistence region in between. The data obtained agree well with previous studies of the transition where the standard auxiliary-field quantum Monte Carlo[3] algorithm was used as a solver for DMFT equations (36,37)[7]. Note, CT-QMC scheme gives better accuracy than auxiliary-field quantum Monte Carlo[3] algorithm since one obtains the local Green function at Matsubara frequencies directly in QMC. It allows one to perform simulations at lower temperatures. For instance, we tested the CT-QMC algorithm even at $\beta = 256$ and obtained quite reasonable results for the metal-insulator phase transition on Bethe lattice (see inset for Figure 6 as well).

C. Multi-band model with a rotationally-invariant retarded exchange

Another advantage of the CT-QMC algorithm is that it allows one to consider multi-band problems with interactions in the most general form:

$$\hat{U} = \frac{1}{2} \sum_{ijkl;\sigma\sigma'} U_{ijkl} c^\dagger_{i\sigma} c^\dagger_{j\sigma'} c^{l\sigma'} c^{k\sigma} . \tag{40}$$
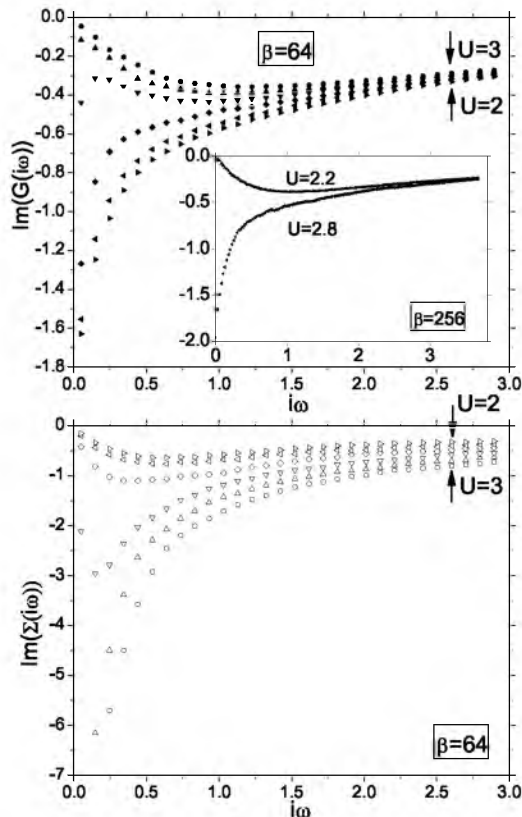
9

FIG. 6: Imaginary part of the Green function (a) and self-energy (b) at Matsubara frequencies for Hubbard model on Bethe lattice at half-filling obtained from the solution of self-consistent DMFT equations (36,37) by CT-QMC method. Parameters: $\beta = 64, U = 2 \div 3, \Delta U = 0.2$. All data obtained with the initial guess for the Green function in the form (38) which corresponds to the metallic phase. Coexistence of metallic and insulating phases can be found, for example, at point $U = 2.4$. Inset shows data for the imaginary part of the Green function for $\beta = 256$, $U = 2.2$ and $U = 2.8$.

We apply the proposed CT-QMC for the important problem of the super-symmetric two band impurity model at half-filling[22,23]. To our knowledge, this is the first successful attempt to take the off-diagonal exchange terms of this model into account. These terms are important for the realistic study of the multi-band Kondo problem because they are responsible for the local moment formation[22]. The interaction in this model has the following form

$$\frac{U}{2}(\hat{N}(\tau)-2)(\hat{N}(\tau)-2)-\frac{J}{2}(\mathbf{S}(\tau)\cdot\mathbf{S}(\tau)+\mathbf{L}(\tau)\cdot\mathbf{L}(\tau)), \quad (41)$$

where $\hat{N}$ is the operator of total number, S and L are total spin and orbital-momentum operators, respectively. The interaction is spin- and orbital- rotationally invari-

ant. The Gaussian part of the action represents the diagonal semicircular density of states[7] with unitary half-band width (38). We used parameters $U = 4, J = 1$ at $\beta = 4$. Figures 7 and 8 present the results for the local Green function $G^{is}_{is}(\tau)$ and the four-point correlator $\chi(\tau - \tau') =< c^{\dagger}_{0\uparrow\tau}c^{0\downarrow\tau}c^{\dagger}_{1\downarrow\tau'}c^{1\uparrow\tau'} >$. The later quantity characterizes the spin-spin correlations and would vanish if the exchange were absent.

A modification of this model was also studied where spin-flip operators were replaced with the terms fully non-local in time. For example, operator $c^{\dagger}_{0\uparrow\tau}c^{0\downarrow\tau}c^{\dagger}_{1\downarrow\tau}c^{1\uparrow\tau}$ was replaced with $\beta^{-1}\int d\tau' c^{\dagger}_{0\uparrow\tau}c^{0\downarrow\tau}c^{\dagger}_{1\downarrow\tau'}c^{1\uparrow\tau'}$. As it is pointed in the introduction, the retardation effects in the interaction always appear if certain non-Gaussian degrees of freedom are integrated out. Therefore it is of importance to demonstrate that CT-QMC scheme is able to handle the retarded interaction.

The Green function in the time domain was obtained by a numerical Fourier-transform from the CT-QMC data for $G(i\omega_n)$. For high harmonics the following asymptotic form was used: $-\text{Im}(iw + \epsilon)^{-1}$ with $\epsilon \approx 2.9$. The obtained dependencies are presented in Figure 7. Results for the local and non-local in time spin-flip interactions are shown with solid and dot lines, respectively. It is interesting to note that the Green function is rather insensitive to the details of spin-flip retardation. The maximum-entropy guess for DOS is presented in the inset to Figure 7. Both Green functions are very similar and correspond to qualitatively the same density of states (DOS).

To demonstrate the effects due to retardation we calculated the four-point quantity $\chi(\tau)$. These data are obtained similarly, the difference is that $\chi(i\omega)$ is defined at Bose Matsubara frequencies and obeys a $1/\omega^2$ decay. It turns out that a switch to the non-local in time exchange modifies $\chi(\tau)$ dramatically. The local in time exchange results in a pronounced peak of $\chi(\tau)$ at $\tau \approx 0$, whereas the non-local spin-flip results in almost time-independent spin-spin correlations (Figure 8).

IV. CONCLUDING REMARKS

In conclusion, we have developed a fermionic continuous time quantum Monte Carlo method for general non-local in space-time interactions. It's successfully tested for a number of models.

We demonstrated that for Hubbard-type models the computational time for a single trial step scales similarly to that for the schemes based on a Stratonovich transformation. An important difference occurs however for the non-local interactions. Consider, for example, a system with a large Hubbard U and much smaller but still important Coulomb interatomic interaction. One needs to introduce N^2 auxiliary fields per time slice instead of N to take the long-range forces into account. On the other hand, the complexity of the present algorithm remains
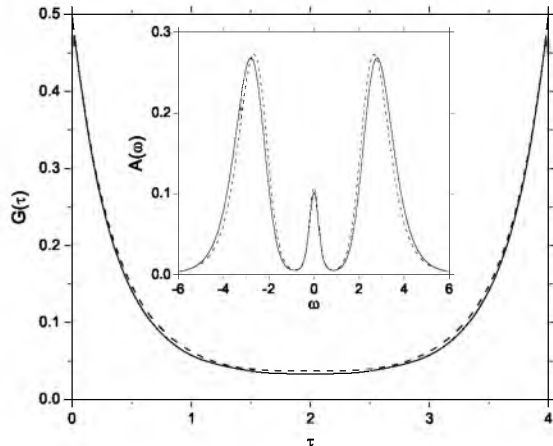
FIG. 7: Imaginary-time Green Function for the rotationally-invariant two-band model. Solid and dot lines correspond to the static and to the nonlocal in time spin-flip, respectively. The inset shows DOS estimated from the Green function.
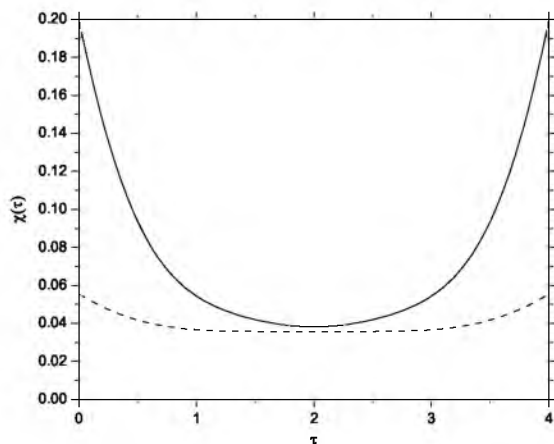

FIG. 8: Imaginary-time dependence of the four-point quantity $\chi(\tau - \tau') = < c^{\dagger}_{0\uparrow\tau} c^{0\downarrow\tau} c^{\dagger}_{1\downarrow\tau'} c^{1\uparrow\tau'} >$ for the rotationally-invariant two-band model. Solid and dot lines correspond to the static and to the nonlocal in time spin-flip, respectively.

almost the same as for the local interactions, because $\overline{|W|}$ does not change much. This should be useful for the realistic cluster DMFT calculations and for the applications to quantum chemistry[5]. It is also possible to study the interactions retarded in time, particularly the super-exchange and the effects related to dissipation. This was demonstrated for an important case of the fully rotationally invariant multi-band model and its extension with non-local in time spin-flip terms.

For the case of the Hubbard model the sign problem was found to be similar to what occurs for the auxiliary-field quantum Monte Carlo[3] scheme. Nevertheless a general time-dependent form of the action (Eq.(2)) opens, in principal, the possibility for a two-stage renormalization treatment. Suppose we know a certain renormalization of action, based on the local DMFT-solution as a starting point. Since DMFT is already a very good approximation, we can expect the thus renormalized interaction to be smaller than the initial one, although it is perhaps nonlocal in time. Then one could expect that the lattice calculations with a renormalized interaction show a smaller sign problem. Practical investigation of such constructed renormalization is a subject of the future work.

* Electronic address: aichten@physnet.uni-hamburg.de

[1] D. J. Scalapino and R.L. Sugar, Phys. Rev. Lett. **46**, 519 (1981).

[2] R. Blankenbecler, D. J. Scalapino, and R. L. Sugar, Phys. Rev. D **24**, 2278 (1981).

[3] J.E. Hirsch, Phys. Rev. B **28**, 4059 (1983); J. E. Hirsch and R. M. Fye, Phys. Rev. Lett. **56**, 2521 (1986).

[4] J. E. Hirsch, Phys. Rev. B **31**, 4403 (1985).

[5] S.R. White J. of Chem. Phys., **117** 7472 (2002).

[6] S.W. Zhang and H. Krakauer, Phys. Rev. Lett. **90**, 136401 (2003).

[7] A. Georges, G. Kotliar, W. Krauth, and M.J. Rozenberg, Rev. Mod. Phys. **68**, 13 (1996).

[8] P. Sun, G. Kotliar Phys. Rev. B **66** 085120 (2002).

[9] M. Capone, M. Fabrizio, C. Castellani, and E. Tosatti Science **296** 2364 (2002).

[10] S. Y. Savrasov, G. Kotliar, and E. Abrahams, Nature **410**, 793 (2001).

[11] A. W. Sandvik and J. Kurkijarvi, Phys. Rev. B **43**, 5950 (1991).

[12] N. V. Prokofev, B. V. Svistunov, and I. S. Tupitsyn, Pisma Zh. Eksp. Teor. Fiz. **64**, 853 (1996) [JETP Lett. **64**, 911 (1996)].

[13] J. Hubbard, Phys. Rev. Lett **3**, 77 (1959), R.L. Stratonovich, Dokl. Akad. Nauk SSSR **115**, 1097 (1957).

[14] M. Troyer, U. J. Wiese cond-mat/0408370.

[15] M. Jarrell,T. Maier, C. Huscroft, and S. Moukouri Phys. Rev. B **64** 195130 (2001).

[16] B. B. Beard and U.-J. Wiese, Phys. Rev. Lett. **77**, 5130 (1996).

[17] P. E. Kornilovitch, Phys. Rev. Lett. **81**, 5382 (1998).

[18] S. M. A. Rombouts, K. Heyde, and N. Jachowicz, Phys. Rev. Lett. **82**, 4155 (1999).

[19] A. N. Rubtsov, cond-mat/0302228; A.N. Rubtsov, A. I. Lichtenstein, JETP Lett. **80** 61 (2004).

[20] G. G. Batrouni and P. de Forcrand, Phys. Rev. B **48**, 589 (1993).

[21] D. R. Hamann and S. B. Fahy, Phys.Rev. B **41**, 11352 (1990).

[22] L. Dworin and A. Narath, Phys. Rev. Lett **1287**, 25 (1970).

[23] M.J. Rozenberg, Phys.Rev. B **55** R4855 (1997)

[24] C. Itzykson, J.-B. Zuber: Quantum Field Theory. McGraw-Hill (1980).